

Tuning zinc doping content to optimize optical and structural properties of $\text{Cd}_{1-x}\text{Zn}_x\text{S}$ buffer layers*

XIE Xin, XUE Yuming**, LÜ Chaoqun, WANG Yifan, WEN Binbin, and WANG Jiangchao

Institute of New Energy Intelligence Equipment, School of Integrated Circuit Science and Engineering, Tianjin University of Technology, Tianjin 300384, China

(Received 23 June 2022; Revised 8 July 2022)

©Tianjin University of Technology 2023

In this paper, $\text{Cd}_{1-x}\text{Zn}_x\text{S}$ thin films were prepared by chemical bath deposition (CBD), and the effects of different zinc doping content on the morphological structure and optical properties of $\text{Cd}_{1-x}\text{Zn}_x\text{S}$ buffer layers are systematically discussed. The experimental results show that in the deposition process of different substrates, the crystal structure of the film is all hexagonal, and when the concentration of zinc sulfate (ZnSO_4) precursor is varied from 0 to 0.025 M, the films are uniform and dense. With the increase of zinc content, the X-ray diffraction (XRD) peak of the films shifted behind that of CdS film (002). It showed 70% to 90% transmittance in the visible region and the optical band gap increased gradually. The band gap value of the films obtained ranged from 2.43 eV to 3.01 eV. It shows the potential feasibility of its application to photovoltaic devices.

Document code: A **Article ID:** 1673-1905(2023)01-0025-6

DOI <https://doi.org/10.1007/s11801-023-2112-3>

The II-VI compound CdS is an n-type semiconductor material, which has been studied as a window layer for heterojunction solar cells for many years^[1]. Due to the narrow band gap of 2.42 eV, the absorption of short wavelengths by the absorber layer is hindered^[2]. ZnS with a large band gap of 3.71 eV^[3] is generally considered to be a substitute for CdS. However, it has poor lattice matching with thin film solar cells of $\text{Cu}(\text{In,Ga})(\text{S,Se})_2$ (CIGS) and CdTe ^[4], which will affect the photoelectric conversion efficiency. In order to obtain semiconductor films with better transparency to match the energy band of the absorber layer, ternary blends with $\text{Cd}_{1-x}\text{Zn}_x\text{S}$ as the buffer layer are investigated in this paper.

Up to now, the main methods to deposit $\text{Cd}_{1-x}\text{Zn}_x\text{S}$ thin films are chemical bath deposition (CBD)^[5], spray pyrolysis^[6], and dipping^[7]. Researchers have explored the properties of $\text{Cd}_{1-x}\text{Zn}_x\text{S}$ thin films by using various deposition methods. ERTURK et al^[8] studied $\text{Cd}_{1-x}\text{Zn}_x\text{S}$ thin films by electrodeposition and performed transmission experiments in the temperature range of 10–300 K. The analytical results showed that the band gap of the films decayed from 2.56 eV to 2.51 eV with increasing temperature. ZELLAGUI et al^[9] prepared $\text{Cd}_{1-x}\text{Zn}_x\text{S}$ thin films by CBD method using cadmium chloride as cadmium source, zinc acetate as zinc source and thiourea as sulfur source, and concluded that higher concentration of cadmium source is favorable for single phase deposition of $\text{Cd}_{1-x}\text{Zn}_x\text{S}$ thin films. MUNNA et al^[10] obtained uni-

formly distributed $\text{Cd}_{1-x}\text{Zn}_x\text{S}$ thin films on the substrate by diluting chemical water bath deposition. The optical band gap of the film increased with increasing zinc source concentration.

Among these deposition techniques, CBD is favored due to its low cost and simple operation. By adjusting the bath conditions, the photoelectric properties of the film can be easily changed and large-area deposition can be achieved. In the classical CBD process, the substrate needs to be immersed in a solution containing zinc salts, cadmium salts, thiourea and ammonia, and at the end of the CBD process, a high concentration of cadmium-containing chemical waste is generated in the plating solution. It is known that cadmium compounds can have harmful effects on health and the environment. We cannot achieve high-quality device performance at the expense of health and the environment.

In this study, zinc sulfate (ZnSO_4) was used as the zinc source, and $\text{Cd}_{1-x}\text{Zn}_x\text{S}$ thin films with similar photoelectric properties to CdS were prepared by CBD method using low concentration cadmium and zinc precursors. This can greatly reduce the output of chemical waste liquid containing cadmium. In addition, $\text{Cd}_{1-x}\text{Zn}_x\text{S}$ was compared with CdS thin films prepared under the same conditions, and the effects of different zinc doping content on the morphology, structure and optical properties of $\text{Cd}_{1-x}\text{Zn}_x\text{S}$ thin films were discussed.

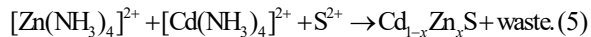
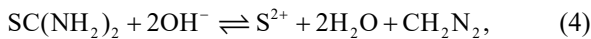
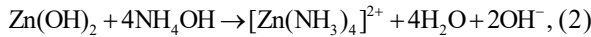
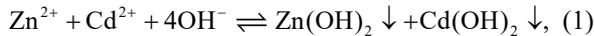
In this experiment, $\text{Cd}_{1-x}\text{Zn}_x\text{S}$ films were deposited on glass and indium tin oxide (ITO) substrates by CBD

* This work has been supported by the Fund for Creative Research Groups.

** E-mail: orwellx@tjut.edu.cn

method. Firstly, the substrates were cleaned with hydrochloric acid, ultrasonic cleaning solution and deionized water and dried with nitrogen. Then they were placed in beakers composed of CdSO_4 (0.005 M), $(\text{NH}_4)_2\text{SO}_4$ (0.015 M), ZnSO_4 with different concentrations and appropriate amount of deionized water. After stirring well with a glass rod, they were put into a constant temperature water bath. The concentration of zinc sulfate in the reaction solution ranged from 0 to 0.025 M. When the water bath was heated to 85°C , ammonia water (25%) and $\text{SC}(\text{NH}_2)_2$ (0.033 M) were added in sequence, and the timing was started, with stirring every 5 min, and a yellow precipitate gradually formed in the beaker. After 35 min of reaction, the beaker was removed, and the sample was rinsed with deionized water and dried with nitrogen.

In this experiment, the presence of Cd^{2+} , Zn^{2+} , and S^{2-} in the solution rapidly produces precipitation due to the small solubility product^[11], which affects the growth of the film. $(\text{NH}_4)_2\text{SO}_4$ complexing agent should be used to reduce the release rate of metal ions. Cd^{2+} and Zn^{2+} react with NH_4^+ to form stable complexes first, and then react with S^{2-} , so that the film deposition rate can be effectively controlled, thus improving the film growth quality. The following chemical reactions occur during the deposition of the film:



The crystal phase structure of the films was analyzed by X-ray diffraction (XRD Rigaku D/max-RB). The Cu target was used, the sample scanning range was $10\text{--}80^\circ$, the step size was 0.02° , the voltage was 40 kV, and the current was 200 mA. The surface morphology, elemental composition and content of the films were analyzed by scanning electron microscope (SEM 460L03040702) and energy dispersive spectrometer (EDS 460L03040702). The absorbance and transmittance of the films in the wavelength range of $300\text{--}800\text{ nm}$ were measured by spectrophotometer (UV-Vis-NIR TP720) and the band gap was calculated.

X-ray diffractometer was used to analyze the structural properties of $\text{Cd}_{1-x}\text{Zn}_x\text{S}$ thin films. Fig.1 shows the XRD patterns of $\text{Cd}_{1-x}\text{Zn}_x\text{S}$ films deposited on different substrates. The diffraction peaks on both bases grow preferentially in the direction of (002). The single peak near 26.6° is considered to be the $\text{Cd}_{1-x}\text{Zn}_x\text{S}$ of hexagonal phase, which is consistent with previous report^[12]. It can be considered that the structure of the $\text{Cd}_{1-x}\text{Zn}_x\text{S}$ thin films prepared by the CBD method is always hexagonal whether on glass or ITO substrate.

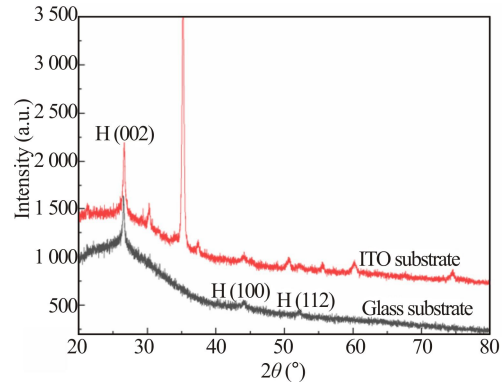


Fig.1 XRD patterns of $\text{Cd}_{1-x}\text{Zn}_x\text{S}$ on different substrates

When another single crystal substance is deposited on a single crystal substrate, the degree of matching of the crystal structure and lattice parameters of the film and substrate can seriously affect the crystal growth behavior of the deposited film. The lattice constants of glass, ITO film, and $\text{Cd}_{1-x}\text{Zn}_x\text{S}$ film are 5.405 nm, 1.011 8 nm, and 0.661 nm, respectively. Bringing them into the mismatch degree equation as^[13]

$$\delta = \frac{2|a_2 - a_1|}{a_2 + a_1}, \quad (6)$$

where a_1 and a_2 are the lattice constants of the two materials (let $a_2 > a_1$), and it can be concluded that the mismatch of $\text{Cd}_{1-x}\text{Zn}_x\text{S}$ -ITO is smaller than that of $\text{Cd}_{1-x}\text{Zn}_x\text{S}$ -glass. The thin film of ITO plays a buffering role between the glass and $\text{Cd}_{1-x}\text{Zn}_x\text{S}$ materials, alleviating the lattice mismatch and improving the quality of the $\text{Cd}_{1-x}\text{Zn}_x\text{S}$ film, so that the intensity of the diffraction peak of the film deposited on the ITO substrate is observed to be higher than that deposited on the glass substrate.

The XRD patterns of $\text{Cd}_{1-x}\text{Zn}_x\text{S}$ films prepared with different concentrations of ZnSO_4 are shown in Fig.2(a). All samples grow preferentially along the hexagonal phase (002) and no peaks corresponding to impurities originating from metals and their oxides and sulfides (Zn, Cd, ZnS, ZnO, CdO) were detected. It is worth noting that the solubility product constant of ZnS is $K_{sp} = 1.4 \times 10^{-24.7}$, while that of CdS is $K_{sp} = 1.4 \times 10^{-29}$ ^[14], so compared with ZnS, the deposition of CdS is performed at lower metal ion concentrations. Therefore, the higher Zn^{2+} concentration in this experiment was not enough to trigger the formation of pristine ZnS nanoparticles.

In order to clearly see the change of the (002) diffraction peak, the XRD pattern at $26\text{--}28^\circ$ was enlarged. As can be seen from Fig.2(b), under the condition of no zinc precursor solution, the CdS film shows diffraction peaks at $2\theta = 26.53^\circ$. After the addition of the zinc precursor solution, the diffraction peak revealed a small shift toward higher angles compared to the CdS peak position at

around $2\theta=26.7^\circ$. This is due to the change in the lattice constant c after zinc doping. According to the Bragg formula $n\lambda=2d\sin\theta$, where λ is the X-ray wavelength, θ is the diffraction angle, and d denotes the crystalline plane distance of indices (h, k, l) . The lattice constant of the CdS film can be calculated by^[15]

$$d_{hkl}^2 = \left[\frac{4(h^2 + k^2 + hk)}{3a^2} + \frac{l^2}{c^2} \right]^{-1}, \quad (7)$$

where a and c are the lattice constants and d_{hkl} is the crystalline plane distance for indices (h, k, l) . According to the equation, the lattice constant of $\text{Cd}_{1-x}\text{Zn}_x\text{S}$ decreases and the increase in the diffraction angle corresponds to a reduction in the lattice plane distance (d_{002}). The ionic radius of Zn^{2+} (0.74 Å) is smaller than that of Cd^{2+} (0.97 Å), and since Cd^{2+} is replaced by Zn^{2+} at its lattice sites, this leads to a decrease in the lattice constant and the (002) lattice plane distance, which is the reason of doping of Zn^{2+} leads to a slight shift of its diffraction angle in a higher direction compared to the CdS film.

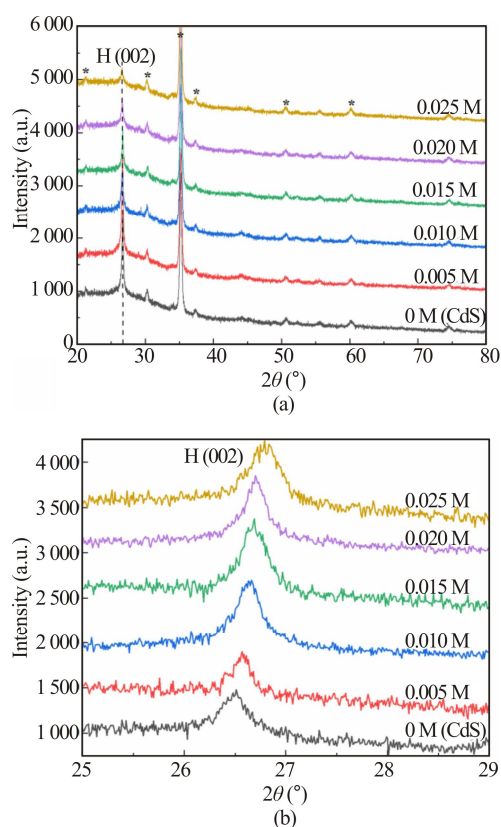


Fig.2 XRD patterns of $\text{Cd}_{1-x}\text{Zn}_x\text{S}$ films as ZnSO_4 concentration varies from 0 to 0.025 M at (a) normal scale and (b) magnified scale for 25° — 29°

In addition to the diffraction peak shift, the width of the main diffraction peak becomes wider and less intense as the zinc salt concentration increases. This indicates that the crystallinity of the film is related to the content of Zn. The higher the content of Zn, the worse the crystallinity of the film. According to the reaction mechanism mentioned above, it can be inferred that when there

is more Zn^{2+} in the reaction solution, these ions preferentially occupy NH_3 to form stable complexes, that is, the formation of Cd^{2+} and NH_3 complex is blocked, and the combination of cadmium ion and sulfur precursor is reduced, so the diffraction peak is reduced.

Fig.3 shows the SEM images of the $\text{Cd}_{1-x}\text{Zn}_x\text{S}$ film, which shows that all films have been formed and nanoparticles are randomly distributed on substrate. When the content of ZnSO_4 is 0—0.010 M (Fig.3(a)—(c)), the films were free of agglomeration, with good film quality and no pores appeared. At 0.015 M ZnSO_4 , the films started to show a few hole defects, and such defects continued to increase at 0.020 M and 0.025 M ZnSO_4 (Fig.3(d)—(f)).

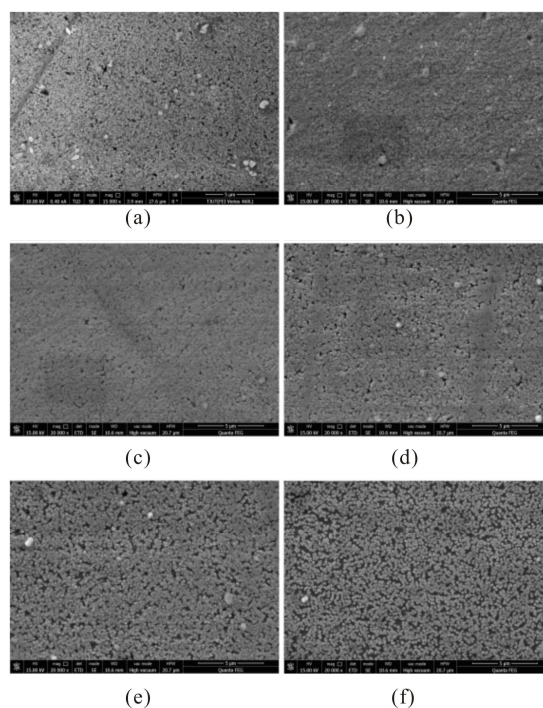


Fig.3 SEM images of $\text{Cd}_{1-x}\text{Zn}_x\text{S}$ films deposited with different ZnSO_4 concentrations: (a) 0 M, (b) 0.005 M, (c) 0.010 M, (d) 0.015 M, (e) 0.020 M, and (f) 0.025 M

The composition of $\text{Cd}_{1-x}\text{Zn}_x\text{S}$ under this experiment was examined by EDS. As shown in Fig.4, the classical graphical elements of $\text{Cd}_{1-x}\text{Zn}_x\text{S}$ include cadmium, zinc and sulfur elements. In the reaction solution, the increase of ZnSO_4 concentration makes more zinc doping into the CdS crystal. As shown in Fig.5, the percentage of zinc elements in the $\text{Cd}_{1-x}\text{Zn}_x\text{S}$ film gradually increases, while the percentage of cadmium elements gradually decreases. Increasing concentration of zinc salts precursors makes the related reactions move in a positive direction and accelerates the rate of metal ion release. As a result, the rate of $\text{Cd}(\text{OH})_2$ and $\text{Zn}(\text{OH})_2$ precipitation in solution is faster than that of $\text{Cd}_{1-x}\text{Zn}_x\text{S}$ film formed by Zn^{2+} , Cd^{2+} , and S^{2-} , that is, the growth rate of $\text{Cd}_{1-x}\text{Zn}_x\text{S}$ film is slower^[16], so the film becomes less dense and holes appear. Since holes will increase the probability of carrier

recombination and reduce the photoelectric conversion efficiency, films with fewer surface holes and better density are more suitable for thin film buffer layers. Therefore, it is concluded that the content of zinc will affect the surface morphology of the film, and with the increase of zinc content, the density of the film becomes worse and the pores increase.

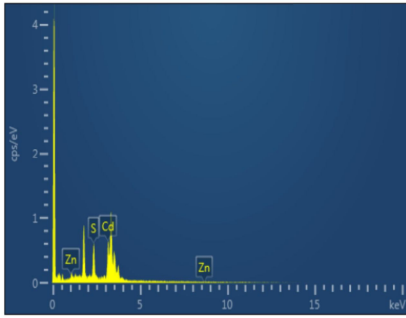


Fig.4 Total spectrum of Cd_{1-x}Zn_xS surface

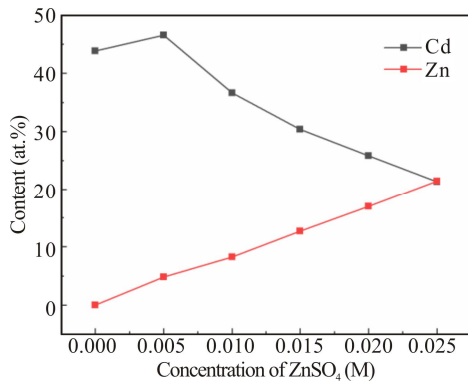


Fig.5 Trend graph of Zn and Cd contents

The optical properties of the films obtained in this experiment were investigated using a UV-Vis NIR spectrophotometer. As shown in Fig.6(a), the film has a high absorbance for light below 500 nm, and the absorbance drops sharply between 300—350 nm. And for the same wavelength of light, it is obvious that with the increase of Zn²⁺ concentration, the absorbance of Cd_{1-x}Zn_xS films increases compared to CdS films for the same wavelength.

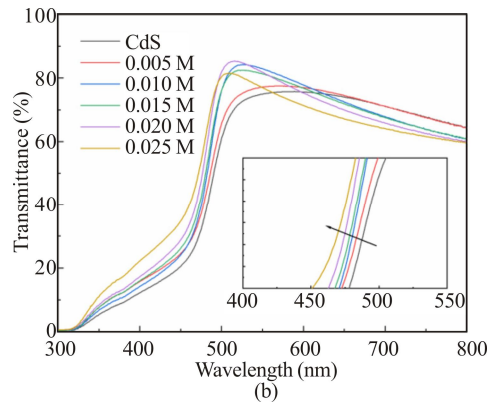
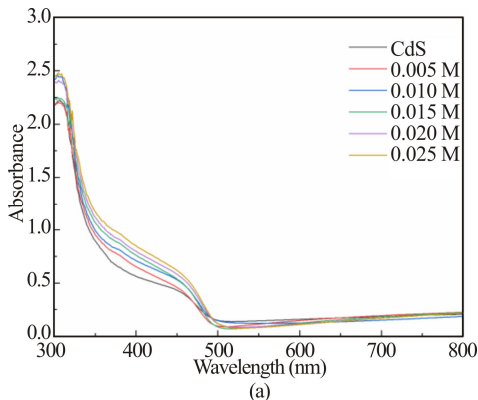


Fig.6 Relationship between absorption, transmittance and wavelength of Cd_{1-x}Zn_xS films with various ZnSO₄ concentrations: (a) Absorption spectra; (b) Transmittance spectra (Inset: the partial enlarged pattern ranging from 400 nm to 550 nm)

To ensure maximum light transmission through the buffer layer to the absorber layer, it is crucial to obtain a film with high transparency. The film transmittance of this experiment is shown in Fig.6(b). The average optical transmittance varies between 70% and 90% in the range of 500—800 nm. With the increase of Zn²⁺ concentration, the film transmittance at 500 nm can reach 88% with superior optical performance. In addition, with the increase of zinc content in the film, the absorption edge appears significantly blue-shifted^[17].

Optical band gap and absorption coefficient of Cd_{1-x}Zn_xS film satisfy Tauc equation as^[18]

$$(\alpha h\nu)^{1/n} = A(h\nu - E_g), \tag{8}$$

where α is the absorption coefficient, $h\nu$ is the photon energy, E_g is the optical band gap of the film, and A is a constant. Since Cd_{1-x}Zn_xS is a direct bandgap semiconductor^[19], the exponent n is taken as 1/2, and the $(\alpha h\nu)^2 - h\nu$ scattering diagram is plotted. By making a tangent line to fit the scattering curve, extending the tangent line to intersect the horizontal axis, and the horizontal coordinate where the tangent line intersects the horizontal axis is the optical band gap of the film. This is shown in Fig.7.

Tab.1 lists the atomic percentages and band gaps of Cd_{1-x}Zn_xS thin films obtained from this experiment. It can be seen intuitively that with the increase of zinc sulfate concentration, the band gap gradually increases, and the change trend of the band gap of the film is consistent with the change trend of zinc content measured by EDS. The increasing trend of the band gap value again verified the substitution effect of zinc on Cd_{1-x}Zn_xS structure.

It was further investigated that there is a certain functional relationship between the zinc content x and the band gap E_g , which can be represented by the dielectric and pseudo potential models^[20]. The relationship between the band gap value and x satisfies

$$E_g(x) = kx^2 + (E_{g(\text{ZnS})} - E_{g(\text{CdS})} - k)x + E_{g(\text{CdS})}, \tag{9}$$

where $E_{g(\text{ZnS})}$ and $E_{g(\text{CdS})}$ denote the bandgap values of CdS and ZnS, and k denotes the bending coefficient. The nonlinear relationship between the bandgap values E_g and x of $\text{Cd}_{1-x}\text{Zn}_x\text{S}$ films for this experiment can be expressed as

$$E_g(x) = 0.32x^2 + 0.96x + 2.43. \quad (10)$$

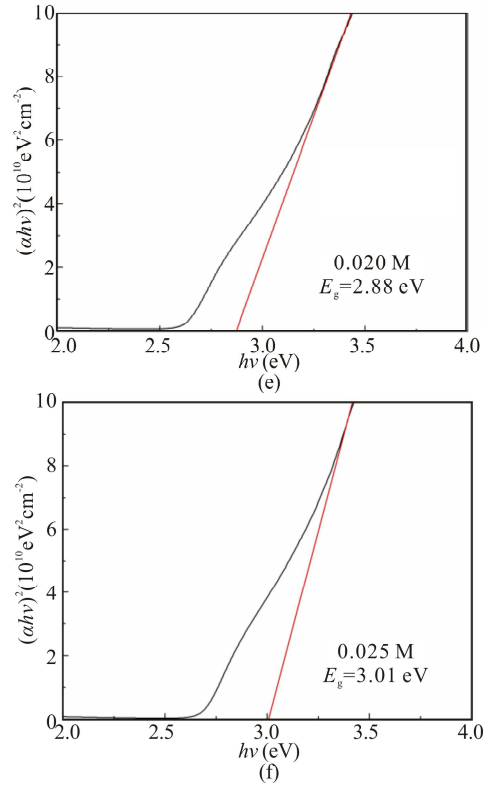
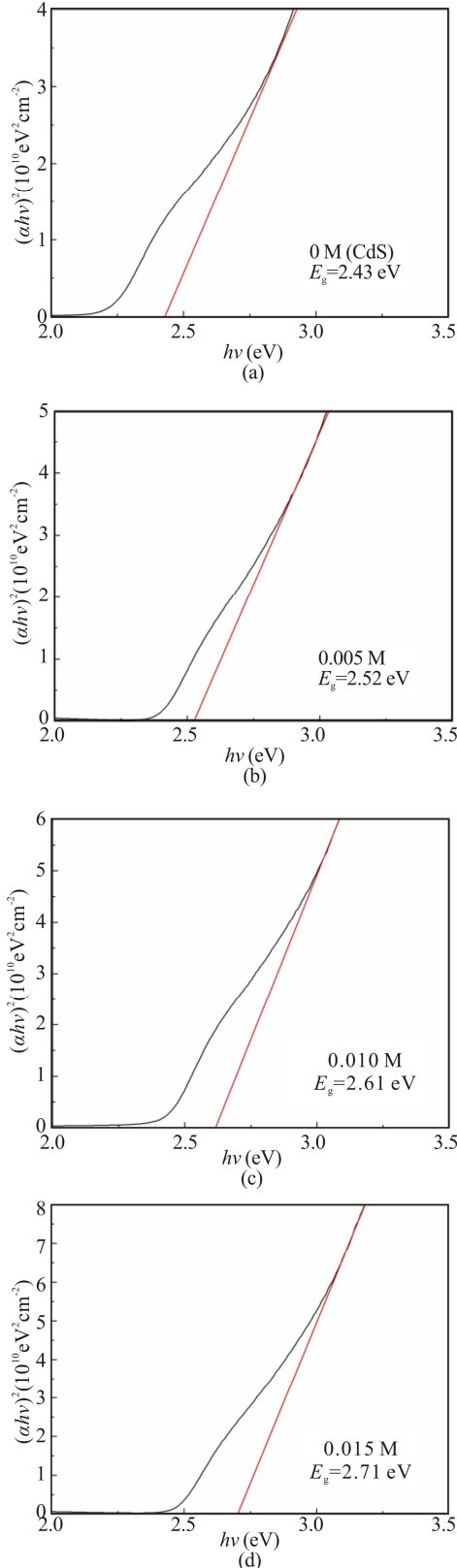


Fig.7 Band gap energy of $\text{Cd}_{1-x}\text{Zn}_x\text{S}$ thin films for different Zn^{2+} concentrations: (a) 0 M, (b) 0.005 M, (c) 0.010 M, (d) 0.015 M, (e) 0.020 M, and (f) 0.025 M

Tab.1 Atomic percentages and band gap of $\text{Cd}_{1-x}\text{Zn}_x\text{S}$

ZnSO_4	S: Zn: Cd (at.%)	Zn: Cd+Zn	$\text{Cd}_{1-x}\text{Zn}_x\text{S}$	E_g
0	56.14:0:43.86	0	CdS	2.43
0.005	48.60:4.81:46.59	0.094	$\text{Cd}_{0.91}\text{Zn}_{0.09}\text{S}$	2.52
0.010	55.09:8.93:35.98	0.199	$\text{Cd}_{0.80}\text{Zn}_{0.20}\text{S}$	2.61
0.015	56.61:12.66:30.37	0.291	$\text{Cd}_{0.71}\text{Zn}_{0.29}\text{S}$	2.71
0.020	57.15:16.41:26.44	0.383	$\text{Cd}_{0.62}\text{Zn}_{0.38}\text{S}$	2.88
0.025	57.24:21.67:21.09	0.507	$\text{Cd}_{0.49}\text{Zn}_{0.51}\text{S}$	3.01

According to Eq.(10), the change of band gap value of $\text{Cd}_{1-x}\text{Zn}_x\text{S}$ film at $0 \leq x \leq 1$ can be obtained, and it can be concluded that increasing the content of zinc in the film will increase the optical band gap of the film. Properly adjusting the proportion of zinc in the film can match the energy bands of the buffer layer and the absorption layer, increase the absorbance of the film, and improve the photoelectric properties of the film.

In this paper, the effect of different zinc doping content on the morphological and optical properties of $\text{Cd}_{1-x}\text{Zn}_x\text{S}$ buffer layer was systematically discussed by combining experiments. The XRD results indicated that with the doping of zinc element, the diffraction peak begins to shift behind the CdS(002) surface, and the higher the zinc content, the worse the crystallinity of the film. The morphological data showed that the growth rate of the films decreased, the thickness became thinner,

the density became worse, and the pores increased with the increase of the proportion of zinc in the films. UV tests revealed that changing the zinc content changed the optical band gap value of the film. With the increase of zinc content and band gap value, the absorbance and transmittance became better. The zinc content and the optical band gap E_g satisfied the equation $E_g(x) = 0.32x^2 + 0.96x + 2.43$. The comprehensive results suggested that 0.010 M $ZnSO_4$ was the ideal concentration for the preparation of $Cd_{0.8}Zn_{0.2}S$ buffer layer. This optimization study provided a guideline for the design and fabrication of buffer layers for future CIGS solar cells.

Statements and Declarations

The authors declare that there are no conflicts of interest related to this article.

References

- [1] GÖDE F, ÜNLÜ S. Synthesis and characterization of CdS window layers for PbS thin film solar cells[J]. *Materials science in semiconductor processing*, 2019, 90: 92-100.
- [2] SHABAN H, GAD S A, MANSOUR B A, et al. The influence of substrate temperatures and thickness on optical and electrical conductivity of $CuIn(Se_{0.25}S_{0.75})_2$ [J]. *Journal of inorganic and organometallic polymers and materials*, 2020, 30(4): 1360-1368.
- [3] WANG L, XUE Y, WANG Z, et al. Effects of ammonia concentration on morphology, composition and optical properties of $ZnO_{1-x}S_x$ thin films of $Cu(In,Ga)Se_2$ solar cells[J]. *Optoelectronics letters*, 2022, 18(4): 0215-0221.
- [4] BARMAN B, BANGERA K V, SHIVAKUMAR G K. A comprehensive study on the structural, morphological, compositional and optical properties of $Zn_xCd_{1-x}S$ thin films[J]. *Materials research express*, 2020, 6(12): 126441.
- [5] MARIAPPAN R, RAGAVENDAR M, PONNUSWAMY V. Growth and characterization of chemical bath deposited $Cd_{1-x}Zn_xS$ thin films[J]. *Journal of alloys and compounds*, 2011, 509(27): 7337-7343.
- [6] BAYKUL M C, ORHAN N. Band alignment of $Cd_{1-x}Zn_xS$ produced by spray pyrolysis method[J]. *Thin solid films*, 2010, 518(8): 1925-1928.
- [7] PATIDAR D, SAXENA N S, SHARMA T P. Structural, optical and electrical properties of CdZnS thin films[J]. *Journal of modern optics*, 2008, 55(1): 79-88.
- [8] ERTURK K, ISIK M, TERLEMEZOGLU M, et al. Optical and structural characteristics of electrodeposited $Cd_{1-x}Zn_xS$ nanostructured thin films[J]. *Optical materials*, 2021, 114: 110966.
- [9] ZELLAGUI R, DEHDOUH H, ADNANE M, et al. $Cd_xZn_{1-x}S$ thin films deposited by chemical bath deposition (CBD) method[J]. *Optik*, 2020, 207: 164377.
- [10] MUNNA F T, SELVANATHAN V, SOBAYEL K, et al. Diluted chemical bath deposition of CdZnS as prospective buffer layer in CIGS solar cell[J]. *Ceramics international*, 2021, 47(8): 11003-11009.
- [11] LILHARE D, KHARE A. Effect of annealing on structural, morphological and optical properties of CdTe/(Cd-Zn)S thin films[J]. *IOP conference series: materials science and engineering*, 2020, 798(1): 012022.
- [12] LIU X, JIANG Y, FU F, et al. Facile synthesis of high-quality ZnS, CdS, CdZnS, and CdZnS/ZnS core/shell quantum dots: characterization and diffusion mechanism[J]. *Materials science in semiconductor processing*, 2013, 16(6): 1723-1729.
- [13] XUE Y, WANG X, ZHANG L, et al. Chemical bath deposition of $Cd_{1-x}Zn_xS$ as buffer layer in CIGS solar cell[J]. *Distributed generation & alternative energy journal*, 2022: 401-418.
- [14] ZHANG L, XUE Y, FENG S, et al. Influence of ammonia concentration on the structural, composition and optical properties of CdZnS thin films[J]. *Materials science in semiconductor processing*, 2019, 104: 104650.
- [15] PUROHIT A, PATEL S L, CHANDER S, et al. Substrate evolution to microstructural and optoelectrical properties of evaporated CdS thin films correlated with elemental composition[J]. *Acta metallurgica sinica (English letters)*, 2021, 34(9): 1307-1316.
- [16] MUNNA F T, CHELVANATHAN P, SOBAYEL K, et al. Effect of zinc doping on the optoelectronic properties of cadmium sulphide (CdS) thin films deposited by chemical bath deposition by utilizing an alternative sulphur precursor[J]. *Optik*, 2020, 218: 165197.
- [17] ZHANG X, CHEN J, CHEN J, et al. Synthesis of CdZnS buffer layer and its impact on $Cu_2ZnSn(S,Se)_4$ thin film solar cells[J]. *Journal of materials science: materials in electronics*, 2022, 33(5): 2399-2405.
- [18] SUN S, GUO J, HAO R, et al. Influence of $Cd_{0.6}Zn_{0.4}S$ buffer layer on the band alignment and the performance of CZTS thin film solar cells[J]. *Optical materials*, 2021, 112: 110666.
- [19] XUE Y, ZHANG S, SONG D, et al. Effect of concentration of cadmium sulfate solution on structural, optical and electric properties of $Cd_{1-x}Zn_xS$ thin films[J]. *Journal of semiconductors*, 2021, 42(11): 112101.
- [20] HOSSAIN T, SOBAYEL M K, MUNNA F T, et al. Tuning the bandgap of $Cd_{1-x}Zn_xS$ ($x=0\sim 1$) buffer layer and CIGS absorber layer for obtaining high efficiency[J]. *Superlattices and microstructures*, 2022, 161: 107100.